Journal of Structural Geology xxx (2013) 1–13

Contents lists available at SciVerse ScienceDirect

Journal of Structural Geology

journal homepage: www.elsevier.com/locate/jsg

Fabric development as the key for forming ductile shear zones and enabling plate tectonics

Laurent G.J. Montési*

Department of Geology, University of Maryland, 237 Regents Drive, College Park, MD 20742, USA

ARTICLE INFO

Article history:
Received 15 December 2011
Received in revised form
21 December 2012
Accepted 23 December 2012
Available online xxx

Keywords:
Ductile shear zone
Localization
Foliation
Phyllosilicates

ABSTRACT

Lithospheric deformation on Earth is localized under both brittle and ductile deformation conditions. As high-temperature ductile rheologies are fundamentally strain-rate hardening, the formation of localized ductile shear zones must involve a structural or rheological change or a change in deformation conditions such as an increase in temperature. In this contribution, I develop a localization potential that quantifies the weakening associated with these changes. The localization potential corresponds to the increase in strain rate resulting from that change under constant stress conditions. I provide analytical expressions for the localization potential associated with a temperature increase, grain size reduction, an increase in water fugacity, melt content, or the abundance of a weak mineral phase. I show that these processes cannot localize deformation from a mantle convection scale (10^3 km) to a ductile shear zone scale (1 km). To achieve this, is it necessary to invoke a structural transition whereby the weak phase in a rock forms interconnected layers. This process is efficient only if one phase is much weaker than the others or if the weakest phase has a highly non-linear rheology. Micas, melt, and fine-grained aggregates – unless dry rheologies are used – have the necessary characteristics. As none of these phases is expected to be present in the dry lithosphere of Venus, this concept can explain why Venus, unlike the Earth, does not display a global network of plate boundaries. The diffuse plate boundary in the Central Indian Ocean may be as yet non-localized because serpentinization has not reached the ductile levels of the lithosphere.

1. Introduction

The formation of ductile shear zones remains an enigma of geology. The structure, geometry, and kinematics of shear zones, or mylonites (e.g., Ramsay, 1980; Passchier and Trouw, 2005) have been well documented but there has been little advance as to their mechanics. The difficulty in understanding shear zone mechanics arises from the fundamentally strain-rate hardening characteristics of rocks that deform in the plastic regime, as repeatedly demonstrated by laboratory experiments (e.g. Evans and Kohlstedt, 1995). Therefore, deformation over wide deformation zones, at a low strain rate, should be favored in the middle to lower crust. Instead of this distributed deformation style, localized shear zones are a common occurrence over a variety of scales including kilometric structures that form major tectonic boundaries (Bak et al., 1975; Hamner, 1988; Vauchez and Tommasi, 2003; Gumiaux et al., 2004).

To compensate for strain-rate hardening, shear zones must be weaker than their surroundings thanks to a different value of some state or structural variable that facilitates continued deformation in previously deformed rocks (Poirier, 1980; White et al., 1980; Montési and Zuber, 2002; Regenauer-Lieb and Yuen, 2004). In the brittle field, localization is often associated with a state variable associated with the failure envelope in elastoplastic materials (Rudnicki and Rice, 1975; Rice, 1976; Needleman and Tvegaard, 1992), the microstructure of a slip surface (Dieterich, 1978, 1979; Ruina, 1983; Dieterich and Kilgore, 1994), or a continuum description of damage (Kachanov, 1986; Lyakhovsky et al., 1997, 2011). In a high temperature plastic regime, the nature of the state variable remains a topic of debate, with most studies focusing on grain size evolution or shear heating (Schmid et al., 1977; Etheridge and Welkie, 1979; Brun and Cobbold, 1980; Fleitout and Froideveau, 1980; Hobbs et al., 1986; Fliervoet et al., 1997; Regenauer-Lieb and Yuen, 1998; Braun et al., 1999; Kaus and Podladchikov, 2006; Crameri and Kaus, 2010; Platt and Behr, 2011a, b). However, I will show that even stronger localization may be expected from the development of a layered fabric.

Ductile shear zones are not only a fundamental feature of terrestrial geology. They may also help to explain the different tectonic regime of various terrestrial planets, especially the lack of plate tectonics on Venus. In the next section, I compare the tectonics of

* Tel.: +1 301 405 7534; fax: +1 301 314 7970.
E-mail address: montesi@umd.edu.

0191-8141/$ – see front matter © 2013 Elsevier Ltd. All rights reserved.
http://dx.doi.org/10.1016/j.jsg.2012.12.011

Earth and Venus to argue that ductile shear zones play a fundamental role in generating plate boundaries on Earth. Then, I develop a technique to estimate how much localization may be expected from a change in state variable in a ductile material. By applying this concept to shear heating, grain size diminution, and fabric evolution, I show that the development of a layered structure has the highest potential to localize deformation. Returning to geodynamic applications, I show that the localization potential is much reduced under the dry conditions of Venus compared to Earth. It is also possible to better understand the presence of a diffuse plate boundary in the Central Indian Ocean if localization by fabric development is taken into account.

2. Plate tectonics and ductile shear zones

The cold and strong outer layer of our planet, the lithosphere, is organized in essentially rigid plates separated by plate boundaries, narrow deformation zones (Isacks et al., 1968; Kreemer et al., 2003). Heat loss is modulated by plate tectonics as cold plates converge and sink into Earth's warmer interior at subduction zones (Korenaga, 2008). To be sustained, this motion must be accompanied by plate creation, which occurs at divergent plate boundaries. The narrow width of plate boundaries implies a reduced resistance to deformation, which is also needed to generate strike-slip plate boundaries (Bercovici et al., 2000). Thus, all three kinds of motion – convergence, divergence, and strike-slip motion – are necessary to form a global plate boundary network and sustain plate tectonics. Plate tectonics require not only sufficient vigorous mantle convection, but also a strong lithosphere with weak, localized, deformation zones (Bercovici et al., 2000; Bercovici, 2003; O'Neill et al., 2007).

Venus is likely active today (Smrekar et al., 2010) but its tectonic style is markedly different from Earth's (Solomon et al., 1992). Only rifts, which accommodate limited plate divergence, resemble terrestrial rifts (Schaber, 1982; Campbell et al., 1984; Stofan et al., 1989; Senske et al., 1991; Foster and Nimmo, 1996). The East African Rift, on Earth, (Fig. 1A) and Devana Chasma, on Venus, (Fig. 1B) are both characterized by ~50 km wide, fault-bounded rift valleys with volcanic edifices. By contrast, strike-slip motion is rare on Venus and accommodates only limited offsets (Koenig and Aydin, 1998; Tuckwell and Ghail, 2003), unlike terrestrial large-offset strike-slip boundaries. Lithospheric shortening on Venus is distributed over vast regions of ridged plains (Fig. 1D) or broad fold belts (Squyres et al., 1992; McGill, 1993; Banerdt et al., 1997), whereas Earth features mainly narrow mountain belts. On Earth, even where shortening is spread over a wide area, like in the Sierra

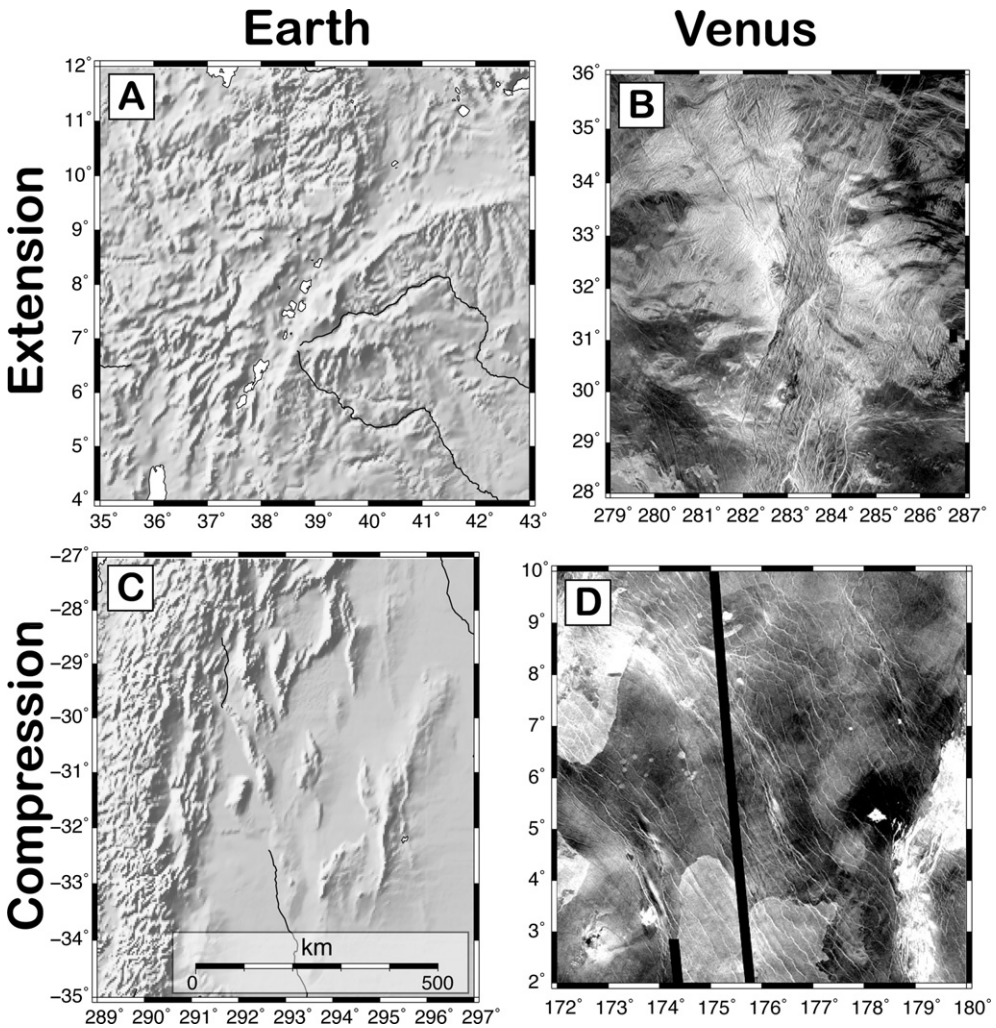

Fig. 1. Comparison of tectonic features on Earth and Venus: A) East African Rift (Ethiopia, Earth); B) Devana Chasma (Beta Regio, Venus); C) Sierra Pampeanas (Argentina, Earth); D) Yalyane Dorsa (Rusalka Planitia, Venus). Earth images are shaded relief from Etopo5 digital elevation model (resolution 5 arc-minutes per pixel) while Venus images are radar mosaics from Magellan data, constructed using the map-a-planet application. Each image covers an 8° × 8° region, displayed at the same scale (panel C).

Please cite this article in press as: Montési, L.G.J., Fabric development as the key for forming ductile shear zones and enabling plate tectonics, Journal of Structural Geology (2013), http://dx.doi.org/10.1016/j.jsg.2012.12.011

Pampaneas (Rodgers, 1987; Jordan and Allmendinger, 1986) in Argentina (Fig. 1C), the spacing of individual uplifts hints at localization of deformation at greater depth than on Venus. Only the Central Indian Basin features a Venus-like, diffuse contractional region (Gordon, 2000). There, seismicity is distributed over more than 1000 km (Weissel et al., 1980). Numerous, basement-cored uplifts and broad folds accommodate limited shortening (Bull and Scrutton, 1990; Chamot-Rooke et al., 1993; Krishna et al., 2001).

As only divergence is localized on Venus, there is no global network of plate boundaries and therefore no plate tectonics. As Earth and Venus have similar heat sources, the difference in tectonic regime must correspond to a difference in the way that the lithosphere deforms. The fine spacing and limited strain of contractional ridges on Venus suggests that localization is limited to a shallow brittle layer (Banerdt et al., 1997). By contrast, terrestrial shear zones extend into the plastic regime, possibly through the entire lithosphere (Sibson, 1977; Scholz, 1988; McBride, 1995; Pili et al., 1997; Wittlinger et al., 1998; Vauchez and Tommasi, 2003; Gumiaux et al., 2004). Therefore, localization in the ductile regime appears necessary to break the entire lithosphere and generate plate boundaries. Therefore, understanding the origin of plate tectonics requires identifying the process that makes plastic localization possible in every geological setting on Earth, but is limited to rifting environments on Venus. It is also important to explain why the deformation area in the Central Indian Basin has not localized into a narrow plate boundary.

Next, I define the localization potential L that quantifies the weakening induced by various structural changes observed in ductile shear zones on Earth. This quantity is used to identify the most likely localization process and describe under what conditions it becomes inefficient.

3. Definition of the localization potential

Structural elements of ductile shear zones that may lead to localization include grain size reduction, development of a layered fabric, metamorphic reactions, and the presence of melts (e.g., Handy et al., 2007; Kelemen and Dick, 1995). Environmental changes, in particular shear heating, have also been suggested (Fleitout and Froidevaux, 1980; Kaus and Podladchikov, 2006).

To quantify the efficiency of these localization process, I define the localization potential, $L = H/h$, where H and h are the widths of deformation zones in a reference and a localized state, respectively (Fig. 2), that necessitate the same stress to deform at a given velocity. The change in material or deformation conditions in the shear zone compared to the reference state increases the strain rate at a given stress, narrowing the deformation zone.

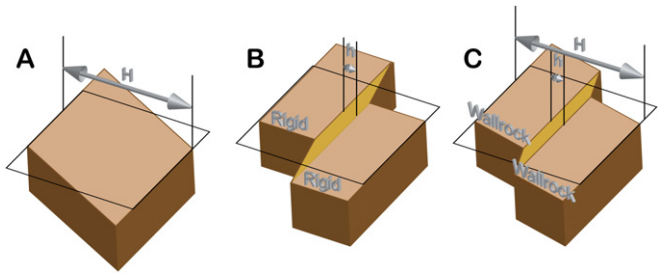

Fig. 2. Schematics diagrams illustrating the reference non-localized deformation state (A) and two localized states: one with rigid wall rock (B), the other with deformable wall rock (C). The different shade of the shear zone in B and C indicates a different temperature or microstructure. The localization potential L is computed by comparing energy dissipation between configurations A and B.

On Earth, distributed deformation zones are ~1000 km wide (Gordon, 2000) whereas ductile shear zones are of order 1 km wide (Vauchez and Tommasi, 2003; Handy et al., 2007). Thus, plate boundary localization requires $L \geq 10^3$. As will be discussed later, higher values of L are actually necessary to explain the development of individual strands of highly sheared material inside individual shear zones.

3.1. Rigid wall rock

The localization potential is calculated by comparing the energy dissipation rate in a reference state, in which deformation is distributed, to that in a perturbed state, in which deformation is localized (Fig. 2). The perturbation could be a difference in the material that is deforming, its constitutive relation, or its deformation environment.

For simplicity, I assume simple shear deformation. In that case, only the shear stress σ and shear strain rate $\dot{\varepsilon}$ need to be considered.

The energy dissipation rate per unit area in the deformation zone is given by

$$\dot{E} = \int_0^H \sigma\dot{\varepsilon}dy = \sigma\int_0^H \dot{\varepsilon}dy = \sigma V \tag{1}$$

where H is the width of the deformation zone and V is the velocity across it. The stress is uniform across the deformation zone under the assumptions that its width is small compared to its area or equivalently that there are no lateral variations in the shear zone width or properties.

The favored state is the one that requires the lowest energy dissipation. For the sake of comparison, I assume that the velocity across the deformation zone is the same in the reference state and in the localization state. Assuming for the time being that the walls of the shear zone are rigid, they contribute to the energy balance. Then, the favored state is also the one with the lowest stress.

In the reference and perturbed states, stress is related to strain rate according to the constitutive relations $\sigma_r(\dot{\varepsilon})$ and $\sigma_p(\dot{\varepsilon})$, respectively. Each is velocity strengthening, meaning that as shear zone width decreases and strain rate increases, stress should also increase. This favors distributed deformation. However, the shear zone, where material or deformation conditions are perturbed, is intrinsically weaker than the reference state. Thus, for a given strain rate, $\sigma_p < \sigma_r$, which favors the perturbed state. The thickness of the deformation zone in the perturbed state decreases, its strain rate increases, and stress increases until it is the same as in the reference state (Tackley, 1998; Platt and Behr, 2011a). Thus, there is a minimum thickness h for which deformation in the perturbed state is favored over deformation in the reference state over a width H. The localization potential is defined as the ratio $L = H/h$.

Computing L is equivalent to determining the strain rate $\dot{\varepsilon}_p$ that, according to the constitutive relation of the perturbed state, requires the same stress as the strain rate $\dot{\varepsilon}_r = V/H$ using the reference constitutive relation. Then, recalling that the velocity across the shear zone is assumed to be the same in localized and distributed states,

$$L = \frac{H}{h} = \frac{\dot{\varepsilon}_p}{\dot{\varepsilon}_r} \tag{2}$$

The localization potential does not consider how the state variable changes from the reference to the localized state, which can be addressed by other analyses (e.g. Rice, 1976; Montési and Zuber, 2002). Because the evolution of state variables can only limit the changes occurring in a deforming rock and the reference state

Please cite this article in press as: Montési, L.G.J., Fabric development as the key for forming ductile shear zones and enabling plate tectonics, Journal of Structural Geology (2013), http://dx.doi.org/10.1016/j.jsg.2012.12.011

ignores preexisting heterogeneities, the localization potential represents the maximum intensity of localization induced by a given change in a state variable. It is unlikely to be fully realized under natural conditions. In addition, as discussed below, deformation in the wall rock of the shear zone also limits localization.

3.2. Deformable wall rocks

The analysis above implies that stress is the same before and after localization, as was also argued by Tackley (1998) and Platt and Behr (2011a). Actually, stress must decrease upon localization because the wall rock is not perfectly rigid. This can be deduced from two separate lines of logic.

In the first scenario, let us assume that the velocity across the shear zone/wall rock system remains V. As the wall rock accommodates deformation, the velocity across the shear zone is less than V. As a consequence, the strain rate and stress in the shear zone are less than expected for the rigid wall rock case, which was shown above as having the same stress as the reference case. Therefore, this situation is inconsistent.

In a second scenario, let us assume that the stress is the same as in the reference state. If the wall rock retains the reference rheology it still deforms at the reference strain rate and the velocity across the model and its total energy would increase by a factor $(2 - 1/L)$, with L defined in Eq. (2). As a consequence, the localized state is unfavorable. Therefore, stress must have decreased to compensate for the velocity increases.

The importance of wall rock deformation can be estimated for a simple model (Fig. 2C) in which the wall rock follow the same rheology as the reference state, and that rheology is a simple power law relation with stress exponent n_w.

$$\dot{\varepsilon}_w = \dot{\varepsilon}_r R^{n_w} \tag{3}$$

with R the ratio of stress in the perturbed and reference states. The shear zone material deforms according to a similar relation but with a potentially different stress exponent n_s and at a faster rate $\dot{\varepsilon}_s$ for a given stress, such that

$$\dot{\varepsilon}_s = L\dot{\varepsilon}_r R^{n_s} \tag{4}$$

where L was defined in Eq. (2) using the rigid walls shear zone model. Then the velocity across the model is $V_l = V_s + V_w = h\dot{\varepsilon}_s + (H - h)\dot{\varepsilon}_w$, where V_s and V_w are the velocities across the shear zone and the wall rocks. Hence:

$$\frac{V_l}{V} = \frac{h}{H} L R^{n_s} + \left(1 - \frac{h}{H}\right) R^{n_w}. \tag{5}$$

where we recall that $\dot{\varepsilon}_r = V/H$. The energy dissipated in the localized state is given by $E_l = R\, V_l\, \sigma$ and it will be less than in the reference state if $V_l/V \leq 1/R$. This leads to the following condition on the thickness of the shear zone:

$$\frac{h}{H} = \frac{1 - R^{n_w+1}}{LR^{n_s+1} - R^{n_w+1}}. \tag{6}$$

This result is similar to Eq. (7) of Tackley (1998), where his fraction W of material that follows the "weak branch" is equivalent to h/H. In term of localization potential, Eq. (6) is equivalent to:

$$L = R^{-n_s-1}\left[\frac{H}{h}\left(1 - R^{n_s+1}\right) + R^{n_w+1}\right]. \tag{7}$$

Eq. (7) is plotted in Fig. 3 for $H/h = 10^3$ that I argued is necessary for the generation of a plate boundary. Although it is impossible to solve independently for H/h and R in general, the properties of Eq. (7) can be understood by examining two limits, small and high stress ratio.

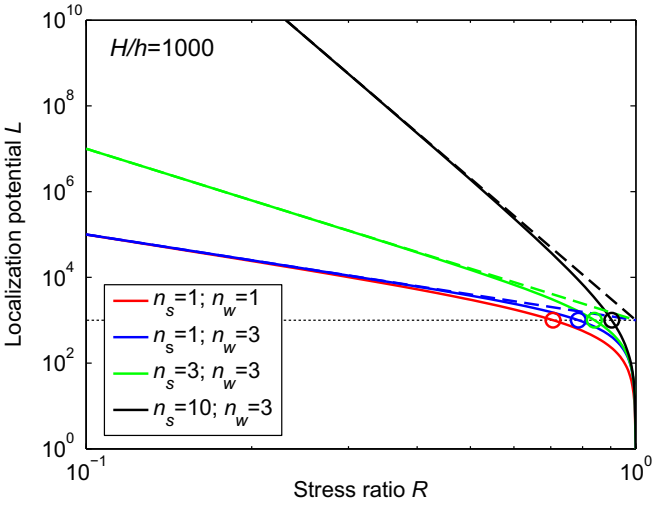

Fig. 3. Localization potential L required to thin a deformation zone by a factor $H/h = 1000$ as a function of the ratio of stress in the localized and in the non-localized state, taking into account wall rock deformation (Fig. 2C). n_s and n_w are the stress exponents of the shear zone and the wall rock, respectively. Dashed lines are the asymptotes for small R (Eq. (8)), which depend only on n_s while the circles mark R for which $L = H/h$.

At small stress ratio $R << 1$:

$$L \approx \frac{H}{h} R^{-n_s-1}. \tag{8}$$

Hence, the localization potential must be much larger than the desired shear zone thickness. Wall rock deformation limits localization and the localization potential must exceed our target value of 10^3 to form a plate boundary. Remarkably, the asymptotic relation in Eq. (8) depends only on shear zone properties.

In the other limit, if $R \sim 1$, the material in the shear zone has almost the same strength as the reference material and it can only occupy a very thin shear zone and velocity across the shear zone is very close to the reference velocity. This model does not result in a significantly higher strain in the shear zone and therefore, although it is mechanically acceptable, it does not describe a geologically important object.

The limit between these two regimes is given by the condition $L = H/h$. In general, the corresponding stress ratio must be solved numerically, but if $n_s = n_w$, we obtain

$$R_c = (2 + 1/L)^{-\frac{1}{n_s+1}} \approx 2^{-\frac{1}{n_s+1}}. \tag{9}$$

where the approximation is done of large localization potential. The critical stress ratio depends principally on shear zone properties (Fig. 3).

In summary, the formation of a geologically significant shear zone occurs only at stress ratios smaller that R_c given by Eq. (9) and requires a localization potential larger than the observed thinning of the deformation zone by approximately a factor R^{-n_s-1} (Eq. (8)). At a minimum, L must exceed $2\ H/h$, possibly more. For simplicity, the following analyses follow the rigid wall approximation but it should be remembered that the localization potential actually needed to form a plate boundary should be larger that the desired H/h ratio of 1000. Supplementary Table 1 compiles the various parameters and variables used in these analyses.

Please cite this article in press as: Montési, L.G.J., Fabric development as the key for forming ductile shear zones and enabling plate tectonics, Journal of Structural Geology (2013), http://dx.doi.org/10.1016/j.jsg.2012.12.011

4. Localization in monomineralic aggregates

4.1. Shear heating

Shear zones are often proposed to form through shear heating. As ductile deformation is temperature-activated and deformation generates heat, a feedback loop may develop whereby heating weakens the material and increases the deformation rate, which generates more heat (Brun and Cobbold, 1980; Fleitout and Froidevaux, 1980; Hobbs et al., 1986; Bai and Dodd, 1992; Regenauer–Lieb and Yuen, 1998, 2004; Kaus and Podladchikov, 2006; Crameri and Kaus, 2010).

The temperature dependence of ductile creep typically follows an Arrhenius-type relation (e.g., Evans and Kohlstedt, 1995):

$$\dot{\varepsilon} = A\sigma^n \exp\left(-\frac{Q}{RT}\right) \tag{10}$$

where n is the stress exponent, Q is the activation energy, T is the temperature, R is the gas constant, and A is a pre-exponential factor that may further depend on grain size, water fugacity, etc.

If the temperature is T in the reference state and $T + \Delta T$ in the shear zone, the localization potential is given by

$$L = \frac{\dot{\varepsilon}_l}{\dot{\varepsilon}_d} = \frac{A\sigma^n \exp[-Q/R(T+\Delta T)]}{A\sigma^n \exp[-Q/RT]} = \exp\left[-\frac{Q}{R}\left(\frac{1}{T+\Delta T} - \frac{1}{T}\right)\right]. \tag{11}$$

Remarkably, this expression does not depend on the reference strain rate or stress, only on the activation energy and the reference temperature. This will be true for most other creep laws but not for low temperature creep, for which the activation energy depends on stress (Evans and Kohlstedt, 1995).

Eq. (11) can be inverted to yield the relative temperature change $x = \Delta T/T$ required to obtain a localization potential L

$$\frac{x}{1+x} = \frac{QR}{T} \ln L \tag{12}$$

Furthermore, is the temperature change is small, as we may expect in ductile shear zones,

$$\frac{x}{1+x} \sim x \tag{13}$$

It is straightforward to calculate that temperature increases of the order of 100 K are needed for $L = 10^3$ at the brittle–ductile transition. Accordingly, simulations of simulations by shear heating predict temperature increases in shear zones of more than 100 K (Kaus and Podladchikov, 2006; Crameri and Kaus, 2010).

However, field observations limit heating to less than ~50 K (Brun and Cobbold, 1980; Camacho et al., 2001), which implies L much less than 10^3 (Fig. 4). Therefore, I conclude that shear heating is unlikely to play a major role in localizing ductile deformation. Even when a large temperature anomaly associated with a shear zone is reported, as for the Ailao Shan – Red River shear zone (Leloup and Kienast, 1993; Leloup et al., 2001), coincident shear heating is insufficient to produce the heat anomaly (Gilley et al., 2003). Instead, heat may have been advected from deeper levels of the lithosphere (Leloup and Kienast, 1993). It is possible that numerical simulations that predict shear localization by shear heating are not applicable to natural conditions because they neglect advection of heat by hydrothermal circulation (Saffer et al., 2003).

Shear heating is even less likely to localize deformation on Venus than on Earth because of the high surface temperatures (Fig. 4), although it is possible that heat is retained more efficiently in shear zones of the dry Venusian lithosphere than on Earth.

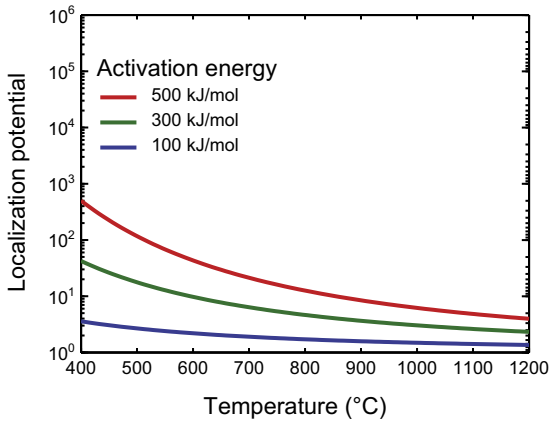

Fig. 4. Localization potential associated with a temperature increase of 50 K in shear zones. The localization potential depends only on temperature and should be at least 10^3 for plate boundary development.

Note that the current analysis is limited to ductile rheologies that follow the template of Eq. (10). Low temperature deformation mechanisms may play a key role in shear heating (Kaus and Podladchikov, 2006). Numerical models and scaling analyses have shown that shear heating can lead to failure of material (Braeck and Podladchikov, 2007) and lithospheric-scale faults in cold cratonic environments under stresses of several hundreds of MPa (Lu et al., 2011). These analyses are compatible the work presented here if localization is defined by a factor of 100 in shear zone width reduction, or if a temperature increase larger than 50 K is allowed. It can also be envisioned that the high temperatures associated with localization in these models are short-lived and do not leave a trace in the rock records. Numerical simulations of spontaneous localization due to shear heating in a high-stress environment have lead to temperature increases high enough to melt rocks (John et al., 2009; Nabelek et al., 2010) and generate earthquake-like shear instabilities (Hobbs et al., 1986; John et al., 2009).

4.2. Change in constitutive relation

The material inside the shear zone may obey a different rheology than the unperturbed material. Assuming that a power law rheology is still appropriate to describe the shear zone rheology, albeit with different constitutive parameters n, A, and Q in the reference and perturbed states, three steps are necessary to compute the localization potential. First, stress is estimated based on the reference state:

$$\sigma = A_r^{-1/n_r} \dot{\varepsilon}_r^{1/n_r} \exp\left(\frac{Q_r}{n_r RT}\right) \tag{14}$$

Then, the localized strain rate is computed

$$\dot{\varepsilon}_l = A_l \sigma^{n_l} \exp\left(-\frac{Q_l}{RT}\right) \tag{15}$$

so that the localization potential is given by

$$L = A_l A_r^{-\frac{n_l}{n_r}} \dot{\varepsilon}^{\frac{n_l}{n_r}} - 1 \exp\left(\frac{n_l Q_r - n_r Q_l}{n_r RT}\right) \tag{16}$$

where the subscripts l and r refer to the localized and reference states, respectively.

Please cite this article in press as: Montési, L.G.J., Fabric development as the key for forming ductile shear zones and enabling plate tectonics, Journal of Structural Geology (2013), http://dx.doi.org/10.1016/j.jsg.2012.12.011

4.2.1. Water fugacity

If the only difference between the reference and perturbed states is due to water fugacity f_{H_2O}, it is sufficient to consider that $A = A_w(f_{H_2O})^{\alpha}$ and

$$L = \left(f_{H_2O_l}/f_{H_2O_r}\right)^{\alpha} \tag{17}$$

As α is close to 1 (Chopra and Paterson, 1984; Mei and Kohlsedt, 2000a, b; Hirth et al., 2001; Hier–Majumder et al., 2005; Rybacki et al., 2006), this effect alone is not sufficient to produce $L \sim 10^3$.

4.2.2. Melting

Partial melts have also been invoked as a weakening agent in rocks. In presence of a small melt fraction ϕ, the strain increases by a factor $\exp(\alpha_m\phi)$.

$$\dot{\varepsilon}_{\phi} = \dot{\varepsilon}_{\phi=0}\exp(\alpha_m\phi) \tag{18}$$

The localization potential associated with a change in melt fraction from ϕ_r to ϕ_l is simply

$$L = \exp[\alpha_m(\phi_l - \phi_r)] \tag{19}$$

Localization is most efficient when $\phi_r = 0$. Even for $\alpha_m = 30$, at the high end of laboratory − determined values (Dell'Angelo and Tullis, 1988; Hirth and Kohlstedt, 1995a, b; Zimmerman and Kohlstedt, 2004), $L = 10^3$ requires $\phi_l > 23\%$, much more than is typically assumed in the partially molten mantle. This value is commensurate with the rheologically critical melt fraction beyond which the partially molten aggregate looses its cohesion and its strength is dominated by the properties of the melt (Arzi, 1978; Lejeune and Richet, 1995; Renner et al., 2000). As melt is much weaker than rocks, a high localization potential is associated with this transition. However, it is unlikely that such high melt fractions would be present over wide regions, based on textural evidence, energy considerations, and on the speed at which melt would escape the system (Sawyer, 1994; Vigneresse et al., 1996; Rosenberg and Handy, 2000). Therefore, localization related to an increase in melt fraction is either episodic (Allibone and Norris, 1992; Handy et al., 2001) or occurs in regions of limited extent. I will return in Section 5.3 to localization involving melt under the assumption that melt is heterogeneously distributed.

4.3. Change in grain size

The most common microstructural characteristic of shear zones is an intense reduction of grain size (e.g. Platt and Behr, 2011b). Because several ductile rheologies, such as diffusion creep, are grain size sensitive, grain size reduction is often considered a likely source of shear zone localization (Schmid et al., 1977; White et al., 1980; Rutter and Brodie, 1988; Knipe, 1990; Drury et al., 1991; Jin et al., 1998; Drury, 2005; Précigout and Gueydan, 2009). However, limits on the conditions for which grain size reduction occurs (De Bresser et al., 1998, 2001; Montési and Hirth, 2003) reduce the likelihood that grain size reduction by itself is responsible for shear zone formation.

Diffusion creep mechanisms may act in parallel with grain-size insensitive dislocation creep leading to the following composite rheology

$$\dot{\varepsilon} = A_{\text{disl}}\sigma^n\exp\left(-\frac{Q_{\text{disl}}}{RT}\right) + A_{\text{diff}}r^{-p}\sigma\exp\left(-\frac{Q_{\text{diff}}}{RT}\right) \tag{20}$$

where r is the grain size and the subscript diff and disl indicate diffusion and dislocation creep coefficients, respectively. A change of grain size from r_d to r_l has a localization potential of

$$L = \frac{1 + \frac{A_{\text{diff}}}{A_{\text{disl}}}r_l^{-p}\sigma^{1-n}\exp\left(\frac{Q_{\text{disl}} - Q_{\text{diff}}}{RT}\right)}{1 + \frac{A_{\text{diff}}}{A_{\text{disl}}}r_d^{-p}\sigma^{1-n}\exp\left(\frac{Q_{\text{disl}} - Q_{\text{diff}}}{RT}\right)} \tag{21}$$

where σ must be computed numerically from Eq. (18) for a given strain rate in the reference state. Fig. 5 shows the localization potential of several rocks types upon reduction of grain size from 1 mm to 10 μm with $\dot{\varepsilon} = 10^{-15}$ s^{-1}. Rheological parameters are summarized in Table 1. The localization potential is highest at high temperature, because, for a given reference strain rate, the rheology of both the reference and the perturbed states are dominated by diffusion creep.

Eq. (21) is best understood by considering the following three instructive limits.

First, if both grain sizes r_l and r_d are so large that diffusion creep is important in neither state, $L \sim 1$: there is no localization as there is no significant change in the constitutive relation.

Second, if both r_l and r_d are so small that diffusion creep dominates in both states,

$$L \sim (r_d/r_l)^p \tag{22}$$

The localization potential is independent of stress. This is the maximum localization potential associated with a given reduction in grain size. With $p = 3$, large localization potential is possible with relatively modest changes in grain size, but it is unclear that grain size can decreases when diffusion creep dominate (de Bresser et al., 1998, 2001).

Third, if diffusion creep dominates in the localized state but dislocation creep dominates in the distributed state,

$$L = A_{\text{diff}}A_{\text{disl}}^{-\frac{1}{n}}\dot{\varepsilon}^{\frac{1-n}{n}}r_l^{-p}\sigma\exp\left(\frac{Q_{\text{diff}}/n - Q_{\text{diff}}}{RT}\right) \tag{23}$$

which is intermediate between the previous limits. This equation can also be derived from Eq. (16) by considering a change of rheology from dislocation to diffusion creep.

The highest localization potential from grain size reduction occurs when the initial grain size is small enough that grain-size sensitive creep dominates even in the reference state. However, these conditions would not be inductive to grain size reduction (de Bresser et al., 1998, 2001), whether reduction is driven by energy dissipation or stress (Kameyama et al., 1997; Braun et al.,

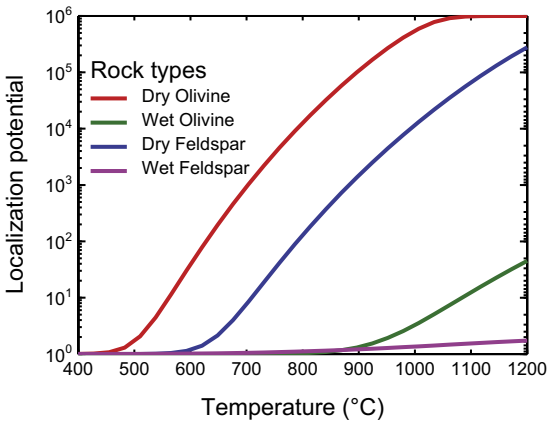

Fig. 5. Localization potential computed for grain size reduction from 1 mm to 10 μm for various rock types (rheological parameters in Table 1), assuming a reference strain rate of 10^{-15} s^{-1}. L should be at least 10^3 for plate boundary development.

Table 1

Rheological parameters; Rock rheology is assumed to obey a power law relationship $\dot{\varepsilon} = A\sigma^n r^{-p} f_{H_2O}^{\alpha} \exp\left(-\frac{Q+PV}{RT}\right)$ with $\dot{\varepsilon}$ the strain rate, σ the stress, r the grain size, f_{H_2O} the water fugacity, P the pressure, R the gas constant, and T the temperature.

Rock	A	n	p	α	$Q + PV$	Comment	Reference
Dry Olivine	1.1×105	3.5	0	0	541	Dislocation creep	Hirth and Kohlstedt (2003)
	1.5×109	1	3	0	381	Diffusion creep	
Wet Olivine	1600	3.5	0	1.2	533	Dislocation creep	
	107.4	1	3	1	387	Diffusion creep	
Dry Feldspar	1012.7	3	0	0	655	Pure anorthite, dislocation creep	Rybacky et al. (2006)
	1012.1	1	3	0	477	Pure anorthite, diffusion creep	
Wet Feldspar	100.2	3	0	1.2	368	Pure anorthite, dislocation creep	
	0.200	1	3	1	182	Pure anorthite diffusion creep	
Dry diabase	195	4.7	0	0	485	Columbia diabase	Mackwell et al. (1998)
Wet diabase	6.12×10^{-2}	3.05	0	0	276		Caristan (1982)
Quartzite	6.31×10^{-12}	4	0	1	135		Hirth et al. (2001)
Biotite	10^{-30}	18	0	0	51		Kronenberg et al. (1990)

1999; Montési and Zuber, 2002; Hall and Parmentier, 2003; Montési and Hirth, 2003; Austin and Evans, 2007). Furthermore, observation of natural shear zones reveal that grain size insensitive dislocation creep typically dominates in the wall rock, with diffusion creep being important only in thin bands of intense grain size reduction (Behrmann and Mainprice, 1987; Warren and Hirth, 2006).

This analysis implies that grain size reduction may be simply an indication of high strain. This makes it a consequence rather than the origin of localization. Indeed several recent studies of shear zones have concluded that variations of grain size in shear reflect original heterogeneities (Warren and Hirth, 2006; Toy et al., 2010; Newman and Drury, 2010) and may not have arisen spontaneously during deformation.

5. Localization in multiphase aggregates

Shear heating and grain size reduction are the principal mechanisms invoked to explain localization in ductile shear zones, but I showed above that their localization potential is probably not high enough to enable the formation of plate boundaries. Other localization processes may be envisioned and, as shown below, are much more efficient. They hinge on the presence of different mineral phases in a deforming rock.

The strength of a polymineralic aggregate depends on the connectivity of weak and strong minerals (Jordan, 1988; Handy, 1990, 1994; Ji et al., 2004; Montési, 2007), which is typically described in relation to two end-member configurations: 1) a dispersed fabric, where strain is uniform and stress is controlled by the most resistant phase, and 2) a layered fabric, where stress is uniform and controlled by the weakest phase (Fig. 6). The analysis that follows shows that, depending upon the minerals involved, the change from a dispersed fabric in the reference state to a layered fabric in shear zone rocks can be associated with an extremely high localization potential (Fig. 7).

5.1. Constitutive relations

When more than one phase is present, the strength of the aggregate depends on the detailed topology of the various phases. The rheology of the aggregate is often described with respect to two idealized configurations (Fig. 6). In the first, the weakest phase occurs in isolated pockets within a framework of strong phase, so that the strain rate is the same in both phases and the stress is

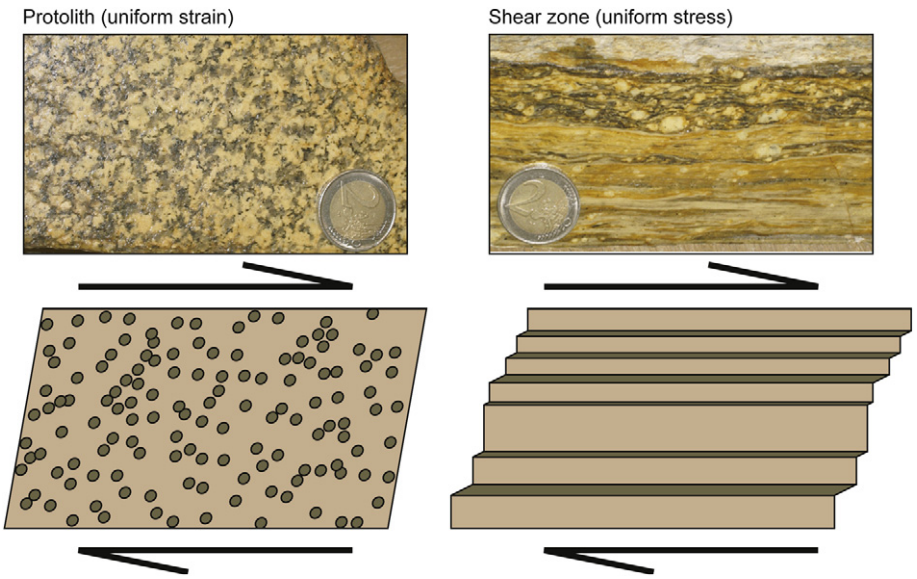

Fig. 6. Typical fabrics of undeformed and shear zone rocks (top), with schematic diagrams (bottom) of the uniform strain (left) and uniform stress (right) configurations that represent their idealized fabrics. Photographs of hand samples of the South Armorican Shear Zone and an undeformed granite found near the shear zone, courtesy of Frédéric Gueydan, University of Montpellier.

Please cite this article in press as: Montési, L.G.J., Fabric development as the key for forming ductile shear zones and enabling plate tectonics, Journal of Structural Geology (2013), http://dx.doi.org/10.1016/j.jsg.2012.12.011

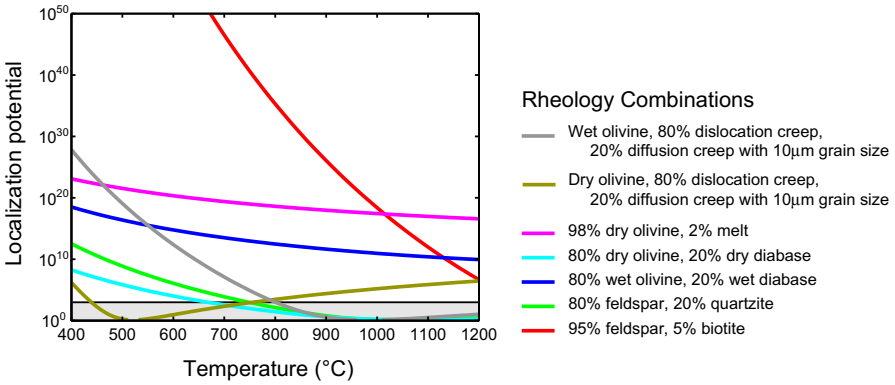

Fig. 7. Localization potential associated with the development of perfect layering and phase separation in aggregates of two materials as indicated in the legend (rheological parameters in Table 1). The reference state has uniform strain in the aggregate and a strain rate of 10^{-15} s^{-1} whereas the shear zone state has uniform stress. The shaded area indicates the conditions for which plate boundary development is not expected ($L \leq 10^3$).

additive. Assuming that each phase obeys a power law creep as in Eq. (10), the aggregates obeys

$$\sigma = (1-C)B_s^{-1/n_s}\dot{\varepsilon}^{1/n_s} + CB_w^{-1/n_w}\dot{\varepsilon}^{1/n_w} \tag{24}$$

where the subscripts w and s correspond to the weak and strong phases, respectively, C is the volume fraction of the multiphase aggregate that is composed of the weak phase, and $B = A\exp(-Q/RT)$.

In the other limit, the weak phase is interconnected and forms layers parallel to the shear direction so that the stress is constant throughout the aggregate but the strain rate is additive throughout the sample. The aggregate obeys

$$\dot{\varepsilon} = (1-C)B_s\sigma^{n_s} + CB_w\sigma^{n_w} \tag{25}$$

These relations can be generalized to more than two phases (Montési, 2007) but this brings unwarranted complexity to the idealized concepts discussed here. Also, it is well known that the strength of most aggregates is intermediate between these end-members (Handy, 1990, 1994; Ji et al., 2004; Gerbi et al., 2010) and is anisotropic (Treagus, 2003; Fletcher, 2004). However, more accurate estimates of the strength of polymineralic aggregates require a detailed description of the topology of the weak and strong phases, which runs against the simplified analysis derived here.

Next, I consider the weakening that may arise 1) as the abundance of the weak phase increases due to syntectonic reactions and 2) as the fabric changes so that the rheology of the reference state is given by Eq. (24) but the rheology of the shear zone is given by Eq. (25).

5.2. Change in weak phase abundance

5.2.1. Layered fabric

Increasing the abundance of weak phase in an aggregate with uniform stress (Eq. (25)) produces the localization potential

$$L = \frac{1 + C_l(R_r - 1)}{1 + C_r(R_r - 1)}, \tag{26}$$

where C_r and C_l are the abundances of weak phase in the reference and perturbed states, respectively, and

$$R_r = \frac{B_w\sigma^{n_w}}{B_s\sigma^{n_s}} \tag{27}$$

is the ratio of strain rate in the weak and strong phases for a stress σ that must first be computed numerically for the reference state (Eq. (25)). For a weak phase, this ratio may be very large.

The special case $C_r = 0$ merits special attention. In that case,

$$L = 1 + C_l(R_r - 1). \tag{28}$$

It has a strong localization potential if the weak phase is very weak, *i.e.*, if the strain rate of the weak phase is much larger than the strain rate of the strong phase at the stress considered.

If $C_r \neq 0$ but the weak phase dominates the strength of the aggregate ($R_r \to +\infty$)

$$L \sim C_l/C_r. \tag{29}$$

As $C_l \leq 1$ per definition, $L \geq 10^3$ requires less than 0.1% initial weak phase abundance.

In either limit, a strong localization potential is possible only if the weak phase is essentially absent in the reference aggregate. However, the analysis assumes that the aggregate is already layered in the reference state, which would be unrealistic with such a low abundance of the weak phase. Therefore, it is unlikely that the change of abundance of a weak phase in a layered aggregate is sufficient to localize global tectonics unto plate boundaries.

5.2.2. Dispersed fabric

If the weak phase is dispersed throughout the aggregate, $L = \dot{\varepsilon}_l/\dot{\varepsilon}_r$, with $\dot{\varepsilon}_l$ computed numerically from Equation (24) under the condition that $\sigma = (1-C_r)B_s^{-1/n_s}\dot{\varepsilon}_r^{1/n_s} + C_rB_w^{-1/n_w}\dot{\varepsilon}_r^{1/n_w}$.

Although it is impossible to obtain an analytical expression for L in the general case, it is instructive to study asymptotic behaviors.

First, let us consider the limit $C_r = 0$. In that case, $\sigma = B_s^{-1/n_s}\dot{\varepsilon}_r^{1/n_s}$ and L is solution of

$$(1-C_l)L^{1/n_s} + CR_s^{-1}L^{1/n_w} = 1 \tag{30}$$

where

$$R_s = \frac{B_s^{-1/n_s}\dot{\varepsilon}_r^{1/n_s}}{B_w^{-1/n_w}\dot{\varepsilon}_r^{1/n_w}} \tag{31}$$

is the ratio of the stresses required to shear the strong and weak phase at the reference strain rate. In the limit that the stress ratio is very high, $R_s >> 1$,

$$L \sim (1-C_l)^{-n_s} \tag{32}$$

The approximate localization potential depends only on the weak phase abundance in the localized state and the stress exponent of the strong phase. As n_s is typically 3, (ref. 2), $L \geq 10^3$ requires that $C \geq 0.9$. In other words sufficient localization is possible only if

Please cite this article in press as: Montési, L.G.J., Fabric development as the key for forming ductile shear zones and enabling plate tectonics, Journal of Structural Geology (2013), http://dx.doi.org/10.1016/j.jsg.2012.12.011

the weak phase is absent in the reference state, makes 90% of the shear zone rock, but never forms an interconnected network. Here again, the necessary fabric is unrealistic and it is unlikely that a change of weak phase abundance in a rock with dispersed fabric is solely responsible for localization of large scale ductile shear zone.

In summary, regardless of the kind of fabric, a change of weak phase abundance without a change of fabric is unlikely to produce enough weakening to localize plate motion over a shear zone width. However, the next section shows that a change from dispersed to layered fabric can.

5.3. Change in type of fabric

When the reference state is associated with the uniform strain rate mixing rheology (Eq. (24)) and the localized state is associated with the uniform stress mixing rheology (Eq. (25), Fig. 6), the localization potential is given by

$$L = (1-C)R_s^{-n_s}[(1-C)R_s + C]^{n_s} + C[(1-C)R_s + C]^{n_w} \tag{33}$$

with C the abundance of weak phase and R_s the initial stress ratio defined in Eq. (31).

An instructive limit is provided by the condition that the strong phase is much stronger than the weak phase, $R_s >> 1$. In that case

$$L \sim C(1-C)R_s^{n_w} \tag{34}$$

This limit can also be computed from Eq. (16) by assuming that the strong phase controls the rheology of the reference state, $\sigma = (1-C)B_s^{-1/n_s}\dot{\varepsilon}_r^{-1/n_s}$, and the weak phase controls the rheology of the localized state, $\dot{\varepsilon}_l = CB_w\sigma^{n_w}$.

Another instructive limit is obtained if the weak phase is rare, $C << 1$,

$$L \sim CR_s^{n_w} \tag{35}$$

regardless of whether the strength contrast R_s is large or small.

In either of these limits, L only depends on the initial strength ratio and on the stress exponent of the weak phase. Intense localization requires either a high strength contrast or a highly nonlinear behavior of the weak phase.

It is possible to identify mineral phases in natural rocks that have the necessary rheological properties (Fig. 7). As most minerals have $n_w \geq 3$, $L = 10^3$ requires $R_s \geq 25$ if $C = 0.5$. That strength contrast is readily achieved the major constituents of the crust. Phyllosilicates result in particularly efficient localization because of their very nonlinear rheology (Kronenberg et al., 1990; Mariani et al., 2006). With $n_w = 10$ and $C = 0.1$, $L = 10^3$ is achieved even for R_s as low as 3. Mariani et al. (2006) argue that strength of mica is essentially independent of strain rate, in which case n_w is infinite and so is the localization potential.

Another intriguing possibility is to consider melt as the weak phase in the rock aggregate. Melt that is present in pore spaces is unlikely to have high crystal content. In that case, it does not have a remarkably highly nonlinear behavior but its viscosity is much less than that of most rock types (e.g. Ryan and Blevins, 1987), leading to a very high localization potential. Evidence of melt impregnation has been reported for many shear zones (Dick, 1977; Hollister and Crawford, 1986; Tommasi et al., 1994; Kelemen and Dick, 1995; Brown and Solar, 1998; Handy et al., 2001; Esteban et al., 2008; Kaczmarek and Müntener, 2008). Highly non-linear behavior of melt is possible at high strain rate, and high crystal content (Caricchi et al., 2007; Deubelbeiss et al., 2011). Although this behavior may lead to localization, it is most appropriate when considering eruptive conditions and probably does not apply to the style of deformation considered here.

The weakening effect of melt can be captured with the exponential strain rate enhancement factor of Eq. (18) (Kohlstedt, 2002). Let us consider a hypothetical rock with an average melt fraction Φ, concentrated into a melt-rich phase with melt fraction ϕ occupying a fraction $C = \Phi/\phi$ of the rock. Fig. 8 presents the localization factor from Eq. (33) for a change of fabric of that rock. Localization can be very high if C is very small, but in that case, ϕ would exceed a rheologically critical melt fraction and Eq. (18) would not be valid. The curves in Fig. 8 terminate where ϕ reaches 25%, at the high end of rheologically critical melt fraction estimates (e.g., Arzi, 1978; Renner et al., 2000). A higher melt content in the weak aggregate is needed if L is to exceed 10^3. As in Section 4.2.2, a high localization potential is possible only if the rheologically critical melt fraction is exceeded. Unlike in Section 4.2.2, a realistic melt fraction of just a few percents may be present on average. At low C, the rheology of the melt-rich regions are dominated by the rheology of the melt phase. Fig. 7 implies that it is possible to have a high localization potential by localizing melt in melt-dominated bands, which would resemble vein or embrittlement features.

Laboratory experiments have shown that interconnection of weak phases such as phyllosilicates can significantly reduce the strength of a mineral aggregate in both semi-brittle (Dell'Angelo and Tullis, 1996; Niemeijer and Spiers, 2005) and fully plastic conditions (Holyoke and Tullis, 2006a, b). In many cases, rock strength is reduced by a factor of two under imposed strain rate conditions in the laboratory and it is possible to capture the strength evolution of the experiment using the mixing rheologies of Eqs. (24) and (25) and a fabric evolution equation (Montési, 2007). In the present analysis, a constant stress is assumed, and L is given by the ratio of strain rate before and after material modification. If the stress exponent of the perturbed material is n_l and the fabric change reduced the rock strength by a factor R, applying the initial stress to the perturbed material would increase strain rate by a factor $L = R^{-n_l}$. Taking $R \sim 1/2$ as in Holyoke and Tullis (2006a) and a conservative $n_l \sim 18$ for strength control by phyllosilicate (Kronenberg et al., 1990), $L \sim 3 \times 10^5$, which is large enough to induce intense localization, although it is less than shown in Fig. 7. This is probably due to an imperfect connection of the weak phase in natural samples.

Under some circumstances, a fine-grained aggregate can play the role of the weak phase and induce intense localization when it forms layers. Fig. 7 presents the localization potential for a mixture of two pseudo-phases, one an aggregate of coarse olivine and the

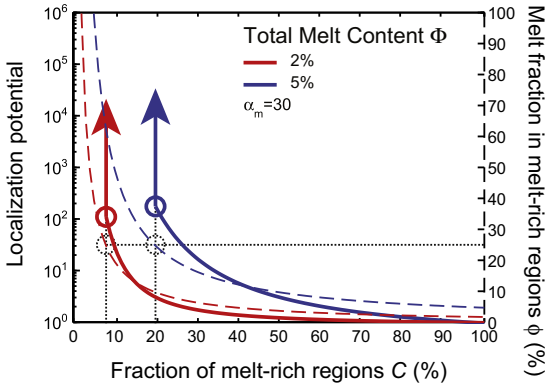

Fig. 8. Localization potential (solid lines) associated with the development of perfect layering and phase separation in aggregates of melt-absent and melt-present olivine ($n = 3.5$). The average melt fraction is 2% or 5% but melt is present only in a fraction C of the aggregate. The dashed line indicates the melt fraction ϕ in the melt-rich regions. The localization potential is computed only when $\phi \leq 25\%$ (circles) and the arrows represent the higher localization potential associated with disaggregation of the melt-rich regions at higher melt content.

Please cite this article in press as: Montési, L.G.J., Fabric development as the key for forming ductile shear zones and enabling plate tectonics, Journal of Structural Geology (2013), http://dx.doi.org/10.1016/j.jsg.2012.12.011

other an aggregate of fine-grained olivine. Although we have seen that a reduction of grain size for the entire rock is associated with a localization potential of less than 10^6, the reorganization of these two phases into shear parallel layers can produce $L \geq 10^{10}$ at low temperature, even if only 20% of the rock is composed of fine-grained olivine and the rheology of fine-grain olivine is linear in this model (Fig. 7).

Grain size reduction and fabric development may reinforce each other to generate shear zones. Rheologies that depend on both grain size and stress dependent, like Dislocation-accommodated Grain Boundary Sliding (Hirth and Kohlstedt, 2003; Warren and Hirth, 2006) and Dynamic Recrystallization (DRX)-assisted dislocation creep (Platt and Behr, 2011b) would probably produce even more localization than shown here. For example, Svahnberg and Piazolo (2010) have shown that the change from dislocation creep in clusters and lenses to Dis-GBS in continuous bands is a central aspect of shear zone development in plagioclase-rich rocks.

6. Applications to large-scale tectonics

In summary, the localization process with the highest potential is the development of a layered fabric when the strength contrast between the strong and weak phases is high, or when the weak phase has a highly nonlinear rheology. In the middle crust, micas, like biotite, act as an efficient localizing phase (Fig. 7), so efficient that it would be unrealistic to assume that the full localization potential is realized, even though the topology of natural shear zones implies a deformation state close to uniform stress (Gerbi et al., 2010). It should be remembered that deformation in the shear zone wall rock is neglected in this analysis. If it is taken into account, the actually localization is much less than the potential, especially if the shear zone material has a strongly non-Newtonian behavior (Fig. 4). In addition, localization is a system-level behavior. The present analysis only describes the effects of a change of state variables, not whether the imposed change is possible. Time-dependent and spatially resolved models are needed to evaluate whether localization will actually occur according to the processes analyzed here.

Only a few combinations of mineral have the right properties to make intense localization possible. Micas do, and are observed to form an interconnected network in many continental ductile shear zones (e.g., Passchier and Trouw, 2005). It is often the case that the phyllosilicate content in a shear zone increases with localization (Mitra, 1978; White and Knipe, 1978; Dixon and Williams, 1983; Wibberley, 1999; Gueydan et al., 2003; Jefferies et al., 2006). Although syntectonic reactions clearly act to weaken the rocks (Brodie and Rutter, 1987; Gueydan et al., 2004; Holyoke and Tullis, 2006b), I have shown that their potential for localization is much less than that due to the development of layers. Therefore, it is appropriate to consider that localization should result from a change in fabric for a constant mineral assemblage.

Clearly, ductile shear zones are not marked only by the presence of layers but also by reduced grain size and higher phyllosilicate abundance compared to the host rock. Increasing the abundance of a weak phase increases the likelihood of that phase forming an interconnected network in the aggregate. Therefore, we should expect a tight coupling between phyllosilicate abundance and rock fabric.

Outside of the continental crust, localization may be possible thanks to other phyllosilicates, as it may be expected that all the minerals in that family share a similar kind of rheology with high anisotropy and highly non-linear behavior. Clays play a key role in explaining the weakness of brittle faults like the San Andreas Fault (Lockner et al., 2011) and fabric has been shown to strongly affect fault strength (Collettini et al., 2009), which is consistent with our analysis. However, in the ductile regime, antigorite is less nonlinear than biotite, with n between 3.4 and 5.8 (Hilairet et al., 2007). Still, antigorite is about two orders of magnitude weaker than olivine under similar conditions, impling $L \sim 10^5$ to 10^{10} (Eq. (34)), which is more than sufficient to induce intense localization.

Importantly, all phyllosilicates dehydrate and break down at temperatures exceeding a few hundreds of degrees. Consequently, the lower lithosphere may not be able to localize because the temperature is too high and phases for which localization by fabric transition is efficient should be absent. This idea can explain the presence of a diffuse plate boundary in the Central Indian Ocean and the absence of plate tectonics on Venus.

In the Central Indian Ocean diffuse plate boundary, localized structures are clearly observed from the surface to the uppermost mantle (Chamot-Rooke et al., 1993). The depth of seismicity (Stein and Weissel, 1990; Petroy and Wiens, 1989) and modeling of tectonic wavelengths (Zuber, 1987; Montési and Zuber, 2003) show that the lithosphere is brittle down to ~40 km. That depth is too great for the lithosphere to be serpentinized during its formation at a mid-ocean ridge (e.g. Iyer et al., 2010). Fluid penetration and serpentinization are ongoing (Verzhbitsky and Lobkovsky, 1993; Delescluse and Chamot-Rooke, 2008) but the brittle–ductile transition is likely at 600 K in this environment, which is too hot for serpentinization. Even if high strain and layering exist locally at the edge of brittle faults, the absence of serpentine may prevent sufficient weakening to generate a narrow plate boundary in spite of ~15 Myr of deformation (Krishna et al., 2009).

Shear zones are observed in exhumed mantle under conditions that have probably involved neither serpentine not melt. Remarkably, stress is estimated to be higher in these shear zones than in the surrounding rock (e.g., Jin et al., 1998). This implies that localization was not a self-sustained spontaneous process but rather that high strain rate was forced upon a given rock mass. This forced localization is expected in the downward continuation of localized shear zones (Montési and Zuber, 2002). Therefore, the mantle lithosphere may be composed of localized brittle faults and serpentine- or melt-lubricated ductile shear zones surrounded by high stress, serpentine- and melt-free ductile shear zones that are not associated with a weakening process and therefore do not participate in rupturing the lithosphere.

Returning to the mineral combinations that are associated with a high localization potential during fabric transition, it is remarkable that dry minerals are systematically associated with lower localization potentials than minerals with water. Micas are hydrated minerals. Localization along bands of fine-grained olivine is efficient only if water-saturated conditions are assumed, as otherwise, L does not exceed 10^6 (Fig. 7). Aggregates of olivine and basalt can produce strong localization if water is present, as there is not a sufficient strength contrast if dry rheologies are employed. Intriguingly, many shear zones in the Earth's lower crust are associated with fluid-induced eclogitization (Austrheim and Griffin, 1985). So, it is fabric development in presence of appropriate rock assemblages, containing fine grained aggregates, phyllosilicates or wet minerals that allows ductile shear zones to develop on Earth.

An interesting corollary to this analysis is that ductile shear zones are difficult to form on Venus. On that planet, localization by shear heating is even less efficient than on Earth because of higher surface temperature. Grain size reduction has been shown above to be limited as a localization process in the absence of coincident fabric development. Very non-linear phases like micas are unlikely on Venus because of the high temperature and the suspected dryness of the lithosphere (Kaula, 1999). On Venus, only melt provides a high localization potential (Fig. 7). Melt-impregnated shear zones are a common occurrence on Earth (Dick, 1977; Brown and Solar, 1998). As melt is most abundant in rifting environments, it can be supposed that the reason why Venusian rifts are

Please cite this article in press as: Montési, L.G.J., Fabric development as the key for forming ductile shear zones and enabling plate tectonics, Journal of Structural Geology (2013), http://dx.doi.org/10.1016/j.jsg.2012.12.011

remarkably Earth-like (Fig. 1) is that melt-impregnated shear zones form at depth and help localize a large-scale rift. As intense localization is unlikely in other tectonic settings on Venus, it is impossible to form a global network of plate boundaries, explaining why plate tectonics is not observed there.

The concepts presented here have implications to early Earth and early Mars. In each case, we have clear evidence for surface water at times when the convective intensity of the planet's interior is intense (e.g., Arndt and Nisbet, 2012; Carr and Head, 2010). If water circulates to sufficient depth into the lithosphere and produces phyllosilicates like mica, it would be expected that plate tectonics is possible then, although issues of lithosphere buoyancy and bending at subduction zones would still have to be resolved (e.g., Korenaga, 2006). On Earth, the evidence for early plate tectonics is highly controversial (Brown, 2008), precluding direct tests of this hypothesis. By contrast, the Martian geological record shows no evidence of plate tectonics even in the earliest epochs. Intriguingly, the clearest evidence for a deep hydrological cycle, provided by mega-outflow channels, is restricted to the Hesperian period, when surface weather is sulfate-dominated (Carr and Head, 2010). It may be speculated that the minerals stable at that time do not have the rheological properties conducive to large-scale localization. However, further work linking the concepts presented here and the feasibility of a global boundary network is clearly needed.

Acknowledgments

This work is supported by grant NASA PGG NNX10AG41G. I thank Maria T. Zuber and Roberta L. Rudnick for their comments on this manuscript as well as Boris Kaus and David Iacoppini for their insightful reviews.

Appendix A. Supplementary data

Supplementary data related to this article can be found at http://dx.doi.org/10.1016/j.jsg.2012.12.011.

References

Allibone, A.H., Norris, R.J., 1992. Segregation of leucogranite microplutons during syn-anatectic deformation: an example from the Taylor Valley, Antarctica. Journal of Metamorphic Geology 10, 589–600.
Arndt, N.T., Nisbet, E.G., 2012. Processes on the young earth and the habitats of early life. Annual Reviews of Earth and Planetary Science 40, 521–549. http://dx.doi.org/10.1146/annurev-earth-042711-105316.
Arzi, A.A., 1978. Critical phenomena in the rheology of partially melted rocks. Tectonophysics 44, 173–184.
Austin, N.J., Evans, B.J., 2007. Paleowattmeters: a scaling relation for dynamically recrystallized grain size. Geology 35, 343–346. http://dx.doi.org/10.1130/G23244A.1.
Austrheim, H., Griffin, W.L., 1985. Shear deformation and eclogite formation within granulite-facies anorthosites of the Bergen Arcs, western Norway. Chemical Geology 50, 267–281.
Bai, Y., Dodd, B., 1992. Adiabatic Shear Localization: Occurrences, Theories, and Applications. Pergamon, New York.
Bak, J., Korstgard, J., Sorensen, K., 1975. A major shear zone within the Nagssugtoquidian of West Greenland. Tectonophysics 27, 191–209.
Banerdt, W.B., McGill, G.E., Zuber, M.T., 1997. Plain tectonics on Venus. In: Bougher, S.W., Hunten, D.M., Phillips, R.J. (Eds.), Venus II. University of Arizona Press, USA, pp. 901–930.
Behrmann, J.H., Mainprice, D., 1987. Deformation mechanisms in a high-temperature quartz-feldspar mylonite: evidence for superplastic flow in the lower continental crust. Tectonophysics 140, 297–305.
Bercovici, D., 2003. The generation of plate tectonics from mantle convection. Earth and Planetary Science Letters 205, 107–121.
Bercovici, D., Ricard, Y., Richards, M.A., 2000. The relation between mantle dynamics and plate tectonics: a primer. In: Richards, M., Gordon, R., van der Hilst, R. (Eds.), The History and Dynamics of Global Plate Motions, Geophysical Monograph, vol. 121. American Geophysical Union, Washington, D.C, pp. 1–46.
Braeck, S., Podladchikov, Y.Y., 2007. Spontaneous thermal runaway as an ultimate failure mechanism of materials. Physical Review Letters 98, 095504. http://dx.doi.org/10.1103/PhysRevLett.98.095504.
Braun, J., Chéry, J., Poliakov, A.N.B., Mainprice, D., Vauchez, A., Tommasi, A., Daignières, M., 1999. A simple parameterization of strain localization in the ductile regime due to grain size reduction: a case study for olivine. Journal of Geophysical Research 104, 25167–25181.
Brodie, K.H., Rutter, E.H., 1987. The role of transiently fine-grained reaction products in syntectonic metamorphism: natural and experimental examples. Canadian Journal of Earth Sciences 24, 556–564.
Brown, M., 2008. Characteristic thermal regimes of plate tectonics and their metamorphic imprint throughout Earth history: when did Earth first adopt a plate tectonics mode of behavior? In: Condie, K.C., Pease, V. (Eds.), When Did Plate Tectonics Begin on Planet Earth? Geological Society of America Special Paper, vol. 440 Geological Society of America, pp. 97–128. http://dx.doi.org/10.1130/2008.2440(05).
Brown, M., Solar, G.S., 1998. Shear-zone systems and melts: feedback relations and self-organization in orogenic belts. Journal of Structural Geology 20, 211–227.
Brun, J.-P., Cobbold, P.R., 1980. Strain heating and thermal softening in continental shear zones: a review. Journal of Structural Geology 2, 149–158.
Bull, J.M., Scrutton, R.A., 1990. Fault reactivation in the central Indian Ocean and the rheology of oceanic lithosphere. Nature 344, 855–858.
Camacho, A., McDougall, I., Armstrong, R., Braun, J., 2001. Evidence for shear heating, Musgrave Block, central Australia. Journal of Structural Geology 23, 1007–1013.
Campbell, D.B., Head, J.W., Harmon, J.K., Hine, A.A., 1984. Venus volcanism and rift formation in Beta Regio. Science 226, 167–170.
Caricchi, L., Burlini, L., Ulmer, P., Gerya, T., Vassalli, M., Papale, P., 2007. New-Newtonian rheology of crystal-bearing magmas and implications for magma ascent dynamics. Earth and Planetary Science Letters 264, 402–419. http://dx.doi.org/10.1016/j.epsl.2007.09.032.
Caristan, Y., 1982. The transition from high temperature creep to fracture in Maryland diabase. Journal of Geophysical Research 87, 6781–6790.
Carr, M.H., Head III, J.W., 2010. Geologic history of Mars. Earth and Planetary Science Letters 294, 185–203. http://dx.doi.org/10.1016/j.epsl.2009.06.042.
Chamot-Rooke, N., Jestin, F., De Voogd, B., 1993. Intraplate shortening in the central Indian Ocean determined from a 2100-km-long north-south deep seismic reflection profile. Geology 21, 1043–1046.
Chopra, P.N., Paterson, M., 1984. The role of water in the deformation of dunite. Journal of Geophysical Research 89, 7861–7876.
Collettini, C., Niemeijer, A., Viti, C., Marone, C., 2009. Fault zone fabric and fault weakness. Nature 462, 907–910. http://dx.doi.org/10.1038/nature08585.
Crameri, F., Kaus, B.J.P., 2010. Parameters that control lithospheric-scale thermal localization on terrestrial planets. Geophysical Research Letters 37, L09308. http://dx.doi.org/10.1029/2010GL042921.
de Bresser, J.H.P., Peach, C.J., Reijs, J.P.J., Spiers, C.J., 1998. On dynamic recrystallization during solid state flow: effects of stress and temperature. Geophysical Research Letters 25, 3457–3460.
de Bresser, J.H.P., ter Heege, J.H., Spiers, C.J., 2001. Grain size reduction by dynamic recrystallization: can it result in major rheological weakening? International Journal of Earth Sciences 90, 28–45.
Delescluse, M., Chamot-Rooke, N., 2008. Serpentinization pulse in the actively deforming Central Indian Ocean. Earth and Planetary Science Letters 276, 140–151. http://dx.doi.org/10.1016/j.epsl.2008.09.017.
Dell'Angelo, L.N., Tullis, J., 1988. Experimental deformation of partially melted granitic aggregates. Journal of Metamorphic Geology 6, 495–515.
Dell'Angelo, L.N., Tullis, J., 1996. Textural and mechanical evolution with progressive strain in experimentally deformed aplite. Tectonophysics 256, 57–82.
Deubelbeiss, Y., Kaus, B.J.P., Connolly, J.A.D., Caricchi, L., 2011. Potential causes for the non-Newtonian rheology of crystal-bearing magmas. Geochemistry Geophysics, Geosystems 12, Q05007. http://dx.doi.org/10.1029/2010GC003485.
Dick, H.J.B., 1977. Evidence of partial melting in the Josephine peridotite. Bulletin of the Oregon State Department of Geology and Mineral Industries 96, 59–62.
Dieterich, J.H., 1978. Time-dependent friction and the mechanics of stick-slip. Pure and Applied Geophysics 116, 790–806.
Dieterich, J.H., 1979. Modeling of rock friction, 1, Experimental results and constitutive equations. Journal of Geophysical Research 84, 2161–2168.
Dieterich, J.H., Kilgore, B.D., 1994. Direct observation of frictional contacts: new insights for sliding memory effects. Pure and Applied Geophysics 143, 283–302.
Dixon, J., Williams, G., 1983. Reaction softening in mylonites from the Arnaboll thrust, Sutherland. Scottish Journal of Geology 19, 157–168.
Drury, M.R., 2005. Dynamic recrystallization and strain softening of olivine aggregates in the laboratory and the lithosphere. In: Gapais, D., Brun, J.P., Cobbold, P.R. (Eds.), Deformation Mechanisms, Rheology and Tectonics: From Minerals to the Lithosphere. Geological Society Special Publication, London, U.K, vol. 243, pp. 127–142.
Drury, M.R., Vissers, R.L.M., van der Wal, C., Hoogerduijn Strating, E.H., 1991. Strain localization in upper mantle peridotites. Pure and Applied Geophysics 137, 439–460. http://dx.doi.org/10.1007/BF00879044.
Esteban, J.J., Cuevas, J., Vegas, N., Tubía, J.M., 2008. Deformation and kinematics in a melt-bearing shear zone from the Western Betic Cordilleras (Southern Spain). Journal of Structural Geology 30, 380–393. http://dx.doi.org/10.1016/j.jsg.2007.11.010.
Etheridge, M.A., Wilkie, J.C., 1979. Grainsize reduction, grain boundary sliding and the flow strength of mylonites. Tectonophysics 58, 159–178.
Evans, B., Kohlstedt, D.L., 1995. Rheology of rocks. In: Ahrens, T.J. (Ed.), Rock Physics and Phase Relations, AGU Reference Shelf 3. American Geophysical Union, Washington, D.C, pp. 143–165.
Fleitout, L., Froideveau, C., 1980. Thermal and mechanical evolution of shear zones. Journal of Structural Geology 2, 159–164.

Fletcher, R.C., 2004. Anisotropic viscosity of a dispersion of aligned elliptical cylindrical clasts in viscous matrix. Journal of Structural Geology 26, 1977–1987. http://dx.doi.org/10.1016/j.jsg.2004.04.004.

Fliervoet, T.F., White, S.H., Drury, M.R., 1997. Evidence for dominant grain-boundary sliding deformation in greenschist- and amphibolite-grade polymineralic ultramylonites from the Redbank Deformed Zone, Central Australia. Journal of Structural Geology 18, 1495–1520.

Foster, A., Nimmo, F., 1996. Comparisons between the rift systems of East Africa, Earth and Beta Regio, Venus. Earth and Planetary Science Letters 143, 183–196.

Gerbi, C., Culshaw, N., Marsh, J., 2010. Magnitude of weakening during crustal-scale shear zone development. Journal of Structural Geology 32, 107–117.

Gilley, L.D., Harrison, T.M., Leloup, P.H., Ryerson, F.J., Lovera, O.M., Wang, J.-H., 2003. Direct dating of left-lateral deformation along the Red River shear zone, China and Vietnam. Journal of Geophysical Research 108, 2127. http://dx.doi.org/10.1029/2001JB001726.

Gordon, R., 2000. Diffuse oceanic plate boundaries: strain rates, vertically averaged rheology, and comparisons with narrow plate boundaries and stable interiors. In: Richards, M., Gordon, R., van der Hilst, R. (Eds.), The History and Dynamics of Global Plate Motions. Geophysical Monograph, vol. 121. American Geophysical Union, Washington, D.C, pp. 143–159.

Gueydan, F., Leroy, Y.M., Jolivet, L., Agard, P., 2003. Analysis of continental midcrustal strain localization induced by microfracturing and reaction-softening. Journal of Geophysical Research 108, 2064. http://dx.doi.org/10.1029/2001JB000611.

Gueydan, F., Leroy, Y.M., Jolivet, L., 2004. Mechanics of low-angle extensional shear zones at the brittle–ductile transition. Journal of Geophysical Research 109, B12407. http://dx.doi.org/10.1029/2003JB002806.

Gumiaux, C., Judenherc, S., Brun, J.-P., Gapais, D., Granet, M., Poupinet, G., 2004. Restoration of lithosphere-scale wrenching from integrated structural and tomographic data (Hercynian belt of Western France). Geology 32, 333–336. http://dx.doi.org/10.1036/G20134.1.

Hall, C.E., Parmentier, E.M., 2003. The influence of grain size on a convective instability. Geochemistry, Geophysics, Geosystems 4, 1029. http://dx.doi.org/10.1029/2002GC000308.

Handy, M.R., 1990. The solid-state flow of polymineralic rocks. Journal of Geophysical Research 95, 8647–8661.

Handy, M.R., 1994. Flow laws for rocks containing two non-linear viscous phases: a phenomenological approach. Journal of Structural Geology 3, 287–301.

Handy, M.R., Mulch, A., Rosenau, M., Rosenberg, C.L., 2001. 2001. The role of fault zones and melt as agents of weakening, hardening, and differentiation of the continental crust: a synthesis. In: Holdsworth, R.E., Strachan, R.A., Magloughlin, J.F., Knipe, R.J. (Eds.), The Nature and Tectonic Significance of Fault Zone Weakening. Geological Society Special Publication, London, U.K., vol. 186, pp. 305–332. http://dx.doi.org/10.1144/GSL.SP.186.01.18.

Handy, M.R., Hirth, G., Bürgmann, R., 2007. Fault structure and rheology from the frictional-viscous transition downward. In: Handy, M.R., Hirth, G., Hovius, N. (Eds.), Tectonic Faults. MIT Press, MA, USA, pp. 139–181.

Hanmer, S., 1988. Great Slave Lake Shear Zone, Canadian Shield: reconstructed vertical profile of a crustal-scale fault zone. Tectonophysics 176, 245–255.

Hier–Majumder, S., Mei, S., Kohlstedt, D.L., 2005. Water weakening of clinopyroxenite in diffusion creep. Journal of Geophysical Research 110, B07406. http://dx.doi.org/10.1029/2004JB003414.

Hilairet, N., Reynard, B., Wang, Y., Daniel, I., Merkel, S., Nishiyama, N., Petitgirard, S., 2007. High-pressure creep of serpentine, interseismic deformation, and initiation of subduction. Science 318, 1910–1913. http://dx.doi.org/10.1126/science.1148494.

Hirth, G., Kohlstedt, D.L., 1995a. Experimental constraints on the dynamics of the partially molten upper mantle 1: deformation in the diffusion creep regime. Journal of Geophysical Research 100, 1981–2001.

Hirth, G., Kohlstedt, D.L., 1995b. Experimental constraints on the dynamics of the partially molten upper mantle 2. Deformation in the dislocation creep regime. Journal of Geophysical Research 100, 15441–15449.

Hirth, G., Kohlstedt, D.L., 2003. Rheology of the upper mantle and the mantle wedge: a view from the experimentalists. In: Eiler, J. (Ed.), The Subduction Factory, Geophysical Monograph, vol. 138. American Geophysical Union, Washington, D.C, pp. 83–105.

Hirth, G., Teyssier, C., Dunlap, W.J., 2001. An evaluation of quartzite flow laws based on comparisons between experimentally and naturally deformed rocks. International Journal of Earth Sciences 90, 77–87.

Hobbs, B.E., Ord, A., Teyssier, C., 1986. Earthquakes in the ductile regime? Pure and Applied Geophysics 124, 309–336.

Hollister, L.S., Crawford, M.L., 1986. Melt-enhanced deformation: a major tectonic process. Geology 14, 558–561.

Holyoke, C.W., Tullis, J., 2006a. Formation and maintenance of shear zones. Geology 34, 105–108. http://dx.doi.org/10.1130/GC22116.1.

Holyoke, C.W., Tullis, J., 2006b. The interaction between reaction and deformation: an experimental study using a biotite + plagioclase +quartz gneiss. Journal of Metamorphic Geology 24, 743–762. http://dx.doi.org/10.1111/j.1525-1314.2006.00666.x.

Isacks, B.L., Oliver, J., Sykes, L.R., 1968. Seismology and the new global tectonics. Journal of Geophysical Research 73, 5855–5899.

Iyer, K., Rüpke, L.H., Phipps Morgan, J., 2010. Feedbacks between mantle hydration and hydrothermal convection at ocean spreading centers. Earth and Planetary Science Letters 296, 34–44. http://dx.doi.org/10.1016/j.epsl.2010.04.037.

Jefferies, S.P., Holdsworth, R.E., Wibberley, C.A.J., Shimamoto, T., Spiers, C.J., Niemeijer, A.R., Lloyd, G.E., 2006. The nature and importance of phyllonite development in crustal-scale fault cores: an example from the Median Tectonic Line, Japan. Journal of Structural Geology 28, 220–235.

Ji, S., Wang, Q., Xia, B., Marcotte, D., 2004. Flow laws for rocks containing two nonlinear viscous phases: a phenomenological approach. Journal of Structural Geology 26, 1377–1390.

Jin, D., Karato, S.-I., Obata, M., 1998. Mechanisms of shear localization in the continental lithosphere: Inference from the deformation microstructures from the Ivrea zone, Northwest Italy. Journal of Structural Geology 20, 195–209.

John, T., Medvedev, S., Rüpke, L.H., Andersen, T.B., Podladchikov, Y.Y., Austrheim, H., 2009. Generation of intermediate-depth earthquakes by self-localizing thermal runaway. Nature Geoscience 2, 137–140. http://dx.doi.org/10.1038/NGEO419.

Jordan, P., 1988. The rheology of polymineralic rocks – an approach. Geologische Rundschau 77, 285–294.

Jordan, T.E., Allmendinger, R.W., 1986. The Sierra Pampeanas of Argentina: a modern analogue of Rocky Mountain foreland deformation. American Journal of Science 286, 737–764.

Kachanov, L.M., 1986. Introduction to Continuum Damage Mechanics. Martinus Nijhoff Publishers, p. 135.

Kaczmarek, M.-A., Müntener, O., 2008. Juxtaposition of melt impregnation and high-temperature shear zones in the upper mantle, field and petrological constraints from the Lanzo peridotite (Northern Italy). Journal of Petrology 40, 2187–2199. http://dx.doi.org/10.1093/petrology/egn065.

Kameyama, M., Yuen, D.A., Fujimoto, H., 1997. The interaction of viscous heating with grain-size dependent rheology in the formation of localized slip zones. Geophysical Research Letters 24, 2523–2526.

Kaula, W.M., 1999. Constraints on Venus evolution from radiogenic Argon. Icarus 139, 32–39.

Kaus, B.K.P., Podladchikov, Y.Y., 2006. Initiation of localized shear zones in viscoplastic rocks. Journal of Geophysical Research 111, B04412. http://dx.doi.org/10.1029/2005JB003652.

Kelemen, P.B., Dick, H.J.B., 1995. Focused melt flow and localized deformation in the upper mantle: juxtaposition of replacive dunite and ductile shear zones in the Josephine peridotite, SW Oregon. Journal of Geophysical Research 100, 423–438.

Knipe, R.J., 1990. Microstructural analysis and tectonic evolution in thrust systems: examples from the Assynt region of the Moine Thrust Zone, Scotland. In: Barber, D.J., Meredith, P.G. (Eds.), Deformation Processes in Mineral, Ceramics, and Rocks. Unwin Hyman, London, pp. 228–261.

Koenig, E., Aydin, A., 1998. Evidence for large-scale strike-slip faulting on Venus. Geology 26, 551–554. http://dx.doi.org/10.1130/0091-7613(1998)026<0551:EFLSSS>2.3.CO;2.

Kohlstedt, D.L., 2002. Partial melting and deformation. In: Karato, S.I., Wenk, H.-R. (Eds.), Plastic Deformation in Minerals and Rocks. Reviews in Mineralogy and Geochemistry, vol. 51. Mineralogical Society of America, Washington, D.C, pp. 105–125.

Korenaga, J., 2006. Archean geodynamics and the thermal evolution of earth. In: Geodynamics, Archean, Environment, Benn K., Mareschal, J.-C., Condie, K.C. (Eds.), Geophysical Monograph, vol. 164. American Geophysical Union, Washington, D.C, pp. 7–32. http://dx.doi.org/10/1029/164GM03.

Korenaga, J., 2008. Urey ratio and the structure and evolution of Earth's mantle. Reviews of Geophysics 46, RG2007. http://dx.doi.org/10.1029/2007RG000241.

Kreemer, C., Holt, W.E., Haines, A.J., 2003. An integrated global model of present-day plate motions and plate boundary deformation. Geophysical Journal International 154, 8–34.

Krishna, K.S., Bull, J.M., Scrutton, R.A., 2001. Evidence for multiphase folding of the central Indian Ocean lithosphere. Geology 29, 715–718.

Krishna, K.S., Bull, J.M., Scrutton, R.A., 2009. Early (pre-8 Ma) fault activity and temporal strain accumulation in the central Indian Ocean. Geology 37, 227–230. http://dx.doi.org/10.1130/G25265A.1.

Kronenberg, A.K., Kirby, S.L., Pinkston, J., 1990. Basal slip and mechanical anisotropy of biotite. Journal of Geophysical Research 95, 19257–19278.

Lejeune, A., Richet, P., 1995. Rheology of crystal-bearing silicate melts: an experimental study at high viscosities. Journal of Geophysical Research 100, 4215–4229.

Leloup, P.H., Kienast, J.R., 1993. High-temperature metamorphism in a major strike-slip shear zone: the Ailao Shan–Red River, People's Republic of China. Earth and Planetary Science Letters 118, 213–234.

Leloup, P.H., Arnaud, N., Lacassin, R., Kienast, J., Harrison, T., Trong, T., Replumaz, A., Tapponnier, P., 2001. New constraints on the structure, thermochronology and timing of the Ailao Shan–Red River shear zone. Journal of Geophysical Research 106, 6683–6732. http://dx.doi.org/10.1029/2000JB900322.

Lockner, D.A., Morrow, C., Moore, D., Hickman, S., 2011. Low strength of the deep San Andreas fault gouge from SAFOD core. Nature 472, 82–85. http://dx.doi.org/10.1038/nature09927.

Lu, G., Kaus, J.P., Zhao, L., 2011. Thermal localization as a potential mechanism to rift cratons. Physics of the Earth and Planetary Interiors 186, 125–137. http://dx.doi.org/10.1016/j.pepi.2011.04.006.

Lyakhovsky, V., Ben-Zion, Y., Agnon, A., 1997. Distributed damage, faulting, and friction. Journal of Geophysical Research 102, 27635–27649.

Lyakhovsky, V., Hamiel, Y., Ben-Zion, Y., 2011. A non-local visco-elastic damage model and dynamic fracturing. Journal of Mechanics and Physics of Solids 59, 1752–1776. http://dx.doi.org/10.1016/j.jmps.2011.05.016.

Mackwell, S., Zimmerman, M., Kohlstedt, D., 1998. High-temperature deformation of dry diabase with application to tectonics on Venus. Journal of Geophysical Research 103, 975–984.

Mariani, E., Brodie, K.H., Rutter, E.H., 2006. Experimental deformation of muscovite shear zones at high temperatures under hydrothermal conditions and the

Please cite this article in press as: Montési, L.G.J., Fabric development as the key for forming ductile shear zones and enabling plate tectonics, Journal of Structural Geology (2013), http://dx.doi.org/10.1016/j.jsg.2012.12.011

strength of phyllosilicate-bearing faults in nature. Journal of Structural Geology 28, 1569–1587.
McBride, J.H., 1995. Does the Great Glen fault really disrupt Moho and upper mantle structure? Tectonics 14, 422–434.
McGill, G.E., 1993. Wrinkle ridges, stress domains, and kinematics of Venusian plains. Geophysical Research Letters 20, 2407–2410.
Mei, S., Kohlstedt, D., 2000a. Influence of water on plastic deformation of olivine aggregates 1. Diffusion creep regime. Journal of Geophysical Research 105, 21457–21469.
Mei, S., Kohlstedt, D., 2000b. Influence of water on plastic deformation of olivine aggregates 2. Dislocation creep regime. Journal of Geophysical Research 105, 21471–21481.
Mitra, G., 1978. Ductile deformation zones and mylonites: the mechanical process involved in the deformation of crystalline basement rocks. American Journal of Science 278, 1057–1084.
Montési, L.G.J., 2007. A constitutive model for layer development in shear zones near the brittle-ductile transition. Geophysical Research Letters 34, L08307. http://dx.doi.org/10.1029/2007GL029250.
Montési, L.G.J., Hirth, G., 2003. Grain size evolution and the rheology of ductile shear zones: from laboratory experiments to postseismic creep. Earth and Planetary Science Letters 211, 97–110. http://dx.doi.org/10.1016/S0012-821X(03)00196-1.
Montési, L.G.J., Zuber, M.T., 2002. A unified description of localization for application to large-scale tectonics. Journal of Geophysical Research 107, 2045. http://dx.doi.org/10.1029/2001JB000465.
Montési, L.G.J., Zuber, M.T., 2003. Spacing of faults at the Scale of the Lithosphere and Localization Instability 2: application to the Central Indian Basin. Journal of Geophysical Research 108, 2111. http://dx.doi.org/10.1029/2002JB001924.
Nabelek, P.I., Whittington, A.G., Hofmeister, A.M., 2010. Strain heating as a mechanism for partial melting and ultrahigh temperature metamorphism in convergent orogens: implications of temperature-dependent thermal diffusivity and rheology. Journal of Geophysical Research 115, B12417. http://dx.doi.org/10.1029/2010JB007727.
Needleman, A., Tvegaard, V., 1992. Analyses of plastic flow localization in metals. Applied Mechanics Reviews 45, S3–S18.
Newman, J., Drury, M.R., 2010. Control of shear zone location and thickness by initial grain size variations in upper mantle peridotites. Journal of Structural Geology 32, 832–842. http://dx.doi.org/10.1016/j.jsg.2010.06.001.
Niemeijer, A.R., Spiers, C.J., 2005. Influence of phyllosilicates on fault strength in the brittle-ductile transition: insights from rock analogue experiments. In: Bruhn, D., Burlini, L. (Eds.), High-strain Zones: Structure and Physical Properties. Geological Society Special Publication, London, U.K, vol. 245, pp. 303–327. http://dx.doi.org/10.1144/GSL.SP.2005.245.01.15.
O'Neill, C., Jellinek, A.M., Lenardic, A., 2007. Conditions for the onset of plate tectonics on terrestrial planets and moons. Earth and Planetary Science Letters 261, 20–32.
Passchier, C.W., Trouw, R.A.J., 2005. Microtectonics. Springer, Berlin, p. 366.
Petroy, D.E., Wiens, D.A., 1989. Historical seismicity and implications for diffuse plate convergence in the northeast Indian Ocean. Journal of Geophysical Research 94, 12301–12319.
Pili, E., Ricard, Y., Lardeayz, J.-M., Sheppard, S., 1997. Lithospheric shear zones and mantle-crust connections. Tectonophysics 280, 15–29.
Platt, J.P., Behr, W.M., 2011a. Lithospheric shear zones as constant stress experiments. Geology 39, 127–130. http://dx.doi.org/10.1130/G31561.1.
Platt, J.P., Behr, W.M., 2011b. Grainsize evolution in ductile shear zones: Implications for strain localization and the strength of the lithosphere. Journal of Structural Geology 33, 537–550. http://dx.doi.org/10.1016/j.jsg.2011.01.018.
Poirier, J.-P., 1980. Shear localization and shear instability in materials in the ductile field. Journal of Structural Geology 2, 135–142.
Precigout, J., Gueydan, F., 2009. Mantle weakening and strain localization: Implications for the long-term strength of the continental lithosphere. Geology 37, 147–150. http://dx.doi.org/10.1130/G25239A.1.
Ramsay, J.G., 1980. Shear zone geometry, a review. Journal of Structural Geology 2, 83–99.
Regenauer-Lieb, K., Yuen, D., 1998. Rapid conversion of elastic energy into shear heating during incipient necking of the lithosphere. Geophysical Research Letters 25, 2737–2740.
Regenauer-Lieb, K., Yuen, D., 2004. Positive feedback of interacting ductile faults from coupling of equations of state, rheology and thermal mechanics. Physics of the Earth and Planetary Interiors 142, 113–135.
Renner, J., Evans, B., Hirth, G., 2000. On the rheologically critical melt fraction. Earth and Planetary Science Letters 181, 585–594.
Rice, J.R., 1976. The localization of plastic deformation. In: Koiter, W.T. (Ed.), Theoretical and Applied Mechanics. North-Holland, New York, pp. 207–220.
Rodgers, J., 1987. Chains of basement uplifts within cratons marginal to orogenic belts. American Journal of Science 287, 661–692.
Rosenberg, C.L., Handy, M.R., 2000. Syntectonic melt pathways during simple shearing of an anatectic rock analogue (norcamphor-benzamide). Journal of Geophysical Research 105, 3135–3149.
Rudnicki, J.W., Rice, J.R., 1975. Conditions for the localization of deformation in pressure-sensitive dilatant materials. Journal of Mechanics and Physics of Solids 23, 371–394.
Ruina, A.L., 1983. Slip instability and state variable friction laws. Journal of Geophysical Research 88, 10359–10370.
Rutter, E.H., Brodie, K.H., 1988. The role of tectonic grain size reduction in the rheological stratification of the lithosphere. Geologische Rundschau 77, 295–308.
Ryan, M.P., Blevins, J.Y.K., 1987. The Viscosity of Synthetic and Natural Silicate Melts and Glasses at High Temperatures and 1 Bar (10^5 Pascals) Pressure and at Higher Pressures. U.S. Geological Survey Bulletin 1764, p. 563.
Rybacki, E., Gottschalk, M., Wirth, R., Dresen, G., 2006. Influence of water fugacity and activation volume on the flow properties of fine-grained anorthite aggregates. Journal of Geophysical Research 111, B03203. http://dx.doi.org/10.1029/2005JB003663.
Saffer, D.M., Bekins, B.A., Hickman, S., 2003. Topographically driven groundwater flow and the San Andreas heat flow paradox revisited. Journal of Geophysical Research 108, 2274. http://dx.doi.org/10.1029/2002JB001849.
Sawyer, E.W., 1994. Melt segregation in the continental crust. Geology 22, 1019–1022.
Schaber, G.G., 1982. Venus: limited extension and volcanism along zones of lithospheric weakness. Geophysical Research Letters 9, 499–502.
Schmid, S.M., Boland, J.N., Paterson, M.S., 1977. Superplastic flow in fine-grained limestone. Tectonophysics 43, 257–291.
Scholz, C.H., 1988. The brittle-plastic transition and the depth of seismic faulting. Geologische Rundschau 7, 319–328.
Senske, D.A., Head, J.W., Stofan, E.R., Campbell, D.B., 1991. Geology and structure of Beta Regio, Venus: results from Arecibo radar imaging. Geophysical Research Letters 18, 1159–1162.
Sibson, R.H., 1977. Fault rocks and fault mechanisms. Journal of the Geological Society, London 133, 191–213.
Smrekar, S.E., Stofan, E.R., Mueller, N., Treiman, A., Elkins-Tanton, L., Helbert, J., Piccione, G., Drossart, P., 2010. Hotspot volcanism on Venus from VIRTIS emissivity data. Science 328, 605–608.
Solomon, S.C., Smrekar, S.E., Bindschadler, D.L., Grimm, R.E., Kaula, W.M., McGill, G.E., Phillips, R.J., Saunders, R.S., Schubert, G., Squyres, S.W., Stofan, E.R., 1992. Venus tectonics: an overview of Magellan observations. Journal of Geophysical Research 97, 13199–13255.
Squyres, S.W., Jankowski, D.G., Simons, M., Solomon, S.C., Hager, B.H., McGill, G.E., 1992. Plains tectonism on Venus: the deformation belts of Lavinia Planitia. Journal of Geophysical Research 97, 13579–13599.
Stein, C.A., Weissel, J.K., 1990. Constraints on the Central Indian Basin thermal structure from heat flow, seismicity, and bathymetry. Tectonophysics 176, 315–332.
Stofan, E.R., Head, J.W., Campbell, D.B., Zisk, S.H., Bogomolov, A.F., Rzhiga, O.N., Basilevsky, A.T., Armand, N., 1989. Geology of a Venus rift zone: Beta Regio and Devana Chasma. Bulletin of the Geological Society of America 101, 143–156.
Svahnberg, H., Piazolo, S., 2010. The initiation of strain localisation in plagioclase-rich rocks: Insights from detailed microstructural analyses. Journal of Structural Geology 32, 1404–1416. http://dx.doi.org/10.1016/j.jsg.2010.06.011.
Tackley, P.J., 1998. Self-consistent generation of tectonic plates in three-dimensional mantle convection. Earth and Planetary Science Letters 157, 9–22. http://dx.doi.org/10.1016/S0012-821X(98)00029-6.
Tommasi, A., Vauchez, A., Fernandes, L.A.D., Porcher, C.C., 1994. Magma-assisted strain localization in an orogen-parallel transcurrent shear zone of southern Brazil. Tectonics 13, 421–437. http://dx.doi.org/10.1029/93TC03319.
Toy, V., Newman, J., Lamb, W., Tikoff, B., 2010. The role of pyroxenites in formation of shear instabilities in the mantle: evidence from an ultramafic ultramylonite, Twin Sisters Massif, Washington. Journal of Petrology 51, 55–80.
Treagus, S.H., 2003. Viscous anisotropy of two-phase composites, and applications to rocks and structures. Tectonophysics 372, 1212–2133. http://dx.doi.org/10.1016/S0040-1951(3)00239-7.
Tuckwell, G.W., Ghail, R.C., 2003. A 400-km-scale strike-slip zone near the boundary of Thetis Regio. Venus. Earth and Planetary Science Letters 211, 45–55. http://dx.doi.org/10.1016/S0012-821X(03)00128-6.
Vauchez, A., Tommasi, A., 2003. Wrench faults down to the asthenosphere: geological and geophysical evidence and thermo-mechanical effects. In: Storti, F., Holdsworth, R.E., Salvini, F. (Eds.), Intraplate Strike-slip Deformation Belts Special Publication, vol. 210. Geological Society, London, U.K, pp. 15–34.
Verzhbitsky, E.V., Lobkovsky, L.I., 1993. On the mechanism of heating-up of the Indo-Australian plate. Journal of Geodynamics 17, 27–38.
Vigneresse, J.L., Barbet, P., Cuney, M., 1996. Rheological transitions during partial melting and crystallization with application to felsic magma segregation and transfer. Journal of Petrology 37, 1579–1600.
Warren, J.M., Hirth, G., 2006. Grain size sensitive deformation mechanisms in naturally deformed peridotites. Earth and Planetary Science Letters 248, 438–450.
Weissel, J.K., Anderson, R.N., Geller, C.A., 1980. Deformation of the Indo-Australian plate. Nature 287, 284–291.
White, S.H., Knipe, R.J., 1978. Transformation- and reaction-enhanced ductility in rocks. Journal of the Geological Society of London 135, 513–516.
White, S.H., Burrows, S.E., Carreras, J., Shaw, N.D., Humphreys, F.J., 1980. On mylonites in ductile shear zones. Journal of Structural Geology 2, 175–187.
Wibberley, C.A.J., 1999. Are feldspar-to-mica reactions necessarily reaction softening process in fault zones. Journal Structural Geology 21, 1219–1227.
Wittlinger, G., Tapponnier, P., Poupinet, G., Mei, J., Danian, S., Herquel, G., Masson, F., 1998. Tomographic evidence for localized lithospheric shear along the AItyn Tagh Fault. Science 282, 74–76.
Zimmerman, M.E., Kohlstedt, D.L., 2004. Rheological properties of partially molten lherzolite. Journal or Petrology 45, 275–298. http://dx.doi.org/10.1093/petrology/egg089.
Zuber, M.T., 1987. Compression of oceanic lithosphere: an analysis of intraplate deformation in the Central Indian Basin. Journal of Geophysical Research 92, 4817–4825.

Please cite this article in press as: Montési, L.G.J., Fabric development as the key for forming ductile shear zones and enabling plate tectonics, Journal of Structural Geology (2013), http://dx.doi.org/10.1016/j.jsg.2012.12.011